Research Article

WIND ENGINEERING

Wind Engineering
2022, Vol. 46(1) 52–68

DOI: 10.1177/0309524X211002833
journals.sagepub.com/home/wie
SAGE

Wind power smoothing in partial load region with advanced fuzzy-logic based pitch-angle controller

Kanasottu Anil Naik[1], Chandra Prakash Gupta[2] and Eugene Fernandez[2]

Abstract

The wind energy system (WES) has an undesirable characteristic in which its power output varies with wind speed, resulting in fluctuations in the grid frequency and voltage. Especially, in partial load region where the wind speed is below rated, there is a concern in regards to WES output power. This part of the work initially employed exponential moving average (EMA) concept to generate reference power. Later on, an interval type-2 fuzzy logic (advanced fuzzy logic) based pitch-angle controller is implemented and designed for good reference tracking and therefore, it can smoothen out the WES output power more effectively. Real time simulations are also developed to show the applicability of the proposed controller using the OPAL-RT digital simulator. Below rated wind speed pattern has considered for real time simulations and results are obtained with different control techniques. The results show that the proposed interval type-2 fuzzy logic (advanced fuzzy logic) based pitch-angle controller offers better performance in tracking reference power and hence, it offers good smoothing of output power fluctuations than conventional proportional-integral (PI) and traditional fuzzy logic (Type-1) controllers. The performance of the proposed controller is also estimated using power smoothing and energy loss functions in terms of performance indices.

Keywords

Wind energy system, power smoothing, pitch-angle control, fuzzy logic controller, uncertainty, Type-2 fuzzy logic controller

Introduction

Wind energy has recently emerged as one of the most promising and significant sources of renewable energy that is replenishable. Unlike conventional power plants, wind power plants emit no air pollutants or greenhouse gases and therefore, wind energy provides clean and non-polluting form of electricity. All these factors have motivated the engineers to adopt the renewable energy resources (The Global Wind Energy Council Belgium, 2016) and today, more than 341,320 wind turbines are spinning all over the world.

Though wind energy is considered to be very prospective source of power generation (Yin, 2018), randomly varying wind speed causes wind power to fluctuate which is still a serious issue for power grids, especially causes voltage (Yin et al., 2015b) and frequency fluctuations. Depending on the wind condition, the wind power fluctuations usually occur on the timescale of a few seconds to several hours. But in case of wind farm, these power fluctuations are smaller as compared to a single WES. However, for isolated systems or future energy system with huge penetration of WESs, it is important to draw attention toward wind power smoothing (Yin et al., 2014a, 2015a, 2016, 2017). However, in case of above rated wind speed the generator output power is limited to its rated value by controlling the pitch angle of the blades. On the other hand, if the wind speed is below rated there is no pitch angle generation and hence maximum power extraction is possible (Yin et al., 2015c, 2015d) as a result, the output power of wind energy system produces fluctuations same as that of the wind speed variations. As the large

[1]Department of Electrical Engineering, National Institute of Technology Warangal, Telangana, India
[2]Department of Electrical Engineering, IIT Roorkee, Roorkee, Uttarakhand, India

Corresponding author:
Kanasottu Anil Naik, Department of Electrical Engineering, National Institute of Technology Warangal, Telangana, India.
Email: anilnaik205@gmail.com

amount of wind farms are realized nowadays and if oscillating output power enter in to the grid lead to grid frequency stability issues.

Many researchers have focused their attention and provided new methods for smoothing the power fluctuations of a wind power system. In Cardenas et al. (2004), smoothing the output power of wind farm has been employed using fly-wheel energy storage system, but it involves a complicated control approach. In Kinjo et al. (2006) and Muyeen et al. (2008), power storage system is studied for smoothing the output power of the WES along-with the wind turbines power quality issues. Though, this method is very effective when the power quality is targeted, but economically not feasible. In Zhang et al. (2005) and Muyeen et al. (2007), a static synchronous compensator (STATCOM) including battery energy storage system (BESS) is employed. However, the BESS application in wind power system is not suggested due to various issues like chemical process involved, short life, and slow response. The superconducting magnetic energy storage (SMES), for their fast response and efficiency, are best choice for wind energy system (Sheikh, et al., 2011). However, with a huge operating cost involved, its application is still critical from a practical point-of-view.

On the other hand, the WT equipped with a pitch-angle controller has become the very popular method for smoothing the output power fluctuations (Yin et al., 2014b, 2015e, 2015f, 2017). Various techniques have been proposed for achieving output power smoothing like H-∞ controller (Sakamoto et al., 2016), adaptive control (Sakamoto et al., 2004), adaptive sliding mode control (Yin et al., 2015g), and predictive control (Senjyu et al., 2006; Yin et al., 2016). However, the main limitation of the H-∞ controllers, they are monolithic and their complexity/order tends to be very high as compared with other controllers. In order to design the adaptive controller a model of the building is necessary and in the case of predictive controller still, there is no industrial development due to implementation issues.

Therefore, intelligent control techniques such as the fuzzy-logic controller (FLC) and fuzzy-NN are implemented in WT pitch-angle controller (Muyeen et al., 2009; Senjyu et al., 2008). These modern techniques have numerous advantages as they do not require the mathematical model of the system and are capable of handling nonlinearity. But, neural network algorithms are complicated and require more intensive computation due to the online training of the system parameters. Therefore, in recent studies (Chowdhury et al., 2012; Duong et al., 2014; Kamel et al., 2010), fuzzy logic controller (called as Type-1 FLC) based pitch-angle controller is best suited as it provides improved performance in tracking reference in comparison to other controllers. Generally, Fuzzy rules and membership functions (MFs) are defined based on experts' knowledge and experience. However, once the membership functions have been defined for designing the controller, the uncertainties in actual degree of MFs cannot be modeled (Hagras and Wagner, 2012). Therefore, there is a need to look for the new methodology to model the uncertainties in the MFs.

Acknowledging the limitations of FLC based pitch-angle controller, this paper proposes an interval Type-2 FLC/advanced fuzzy logic controller (type-2 FLC) based pitch-angle controller to deal with the issues of uncertainty in MFs and Fuzzy rules. The MF of Type-2 fuzzy logic sets (FLSs) is defined with a three-dimensional fuzzy that includes a footprint-of-uncertainty (FOU) (Mendel et al., 2006; Qilian and Mendel, 2000). In the controller design, the third dimension of MFs and FOU offer an additional degree-of-freedom and hence, it is possible to handle and model the uncertainties in the MFs and Fuzzy rules. Therefore, in this work, the FOU has been varied in an appropriate way and an attempt has been made to smoothing the power fluctuations of wind energy system. The contribution of the work lies in designing the Type-2 FLC based pitch angle controller and verified using the real time digital simulator.

Modeling of grid-connected wind energy system

Configuration of the system

The single-line diagram of a typical wind energy system consisting of a wind turbine driven induction generator (IG) is as shown in Figure 1. The stator winding of the IG is connected to the point of common coupling (PCC) through a step-up transformer (0.69/25 kV) which exports power to the 120 kV grid through step-up transformer (25/120 kV) and a transmission line ($R_{TL} + jX_{TL}$) operating at 120 kV. The rotor of the IG is driven by a variable pitch wind turbine. The reactive power absorbed by IG is compensated using capacitor bank (C) connected to the low voltage bus of the wind energy system as shown in Figure 1. The design parameters of the generator and wind turbine are presented in Table A1 & A2 (see Appendix I).

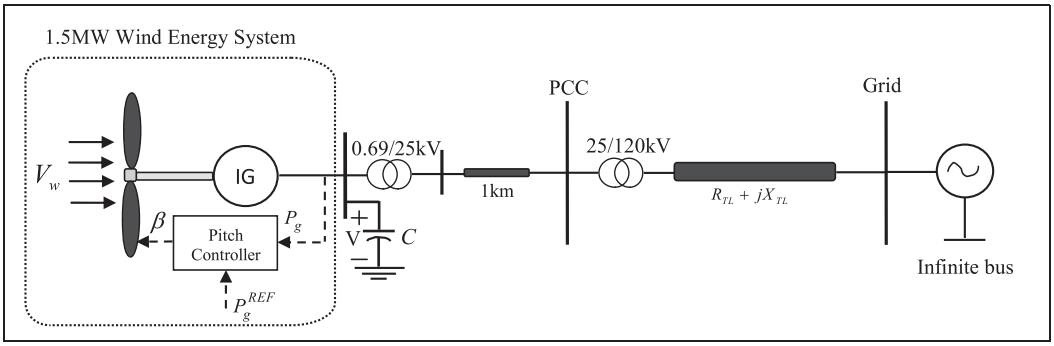

Figure 1. Single-line diagram of the studied grid-connected WES.

Employed wind turbine modeling

The mechanical power developed by a typical wind turbine is directly proportional to the cube of wind speed as

$$P_m = \frac{1}{2}\rho A_r C_p(\lambda,\beta){V_w}^3 = C_p(\lambda,\beta)P_w \tag{1}$$

where P_w is available wind power, ρ is the air-density (kg/m^3), A_r is the turbine swept area (m^2) and can be written as $A_r = \pi R^2$, V_w is the wind speed (m/s), and C_p is the power coefficient.

The typical wind turbine is characterized by the power coefficient (C_p) which depends upon the ratio of rotor-tip speed (λ) and blade pitch-angle (β). The power coefficient (C_p) employed in this study is as follows (Ackerman, 2005):

$$C_p(\lambda,\beta) = c_6\lambda + e^{-c_5/\lambda_i}(-c_4 - c_3\beta + c_2/\lambda_i)c_1 \tag{2}$$

where

$$\frac{1}{\lambda_i} = \frac{1}{0.008\beta + \lambda} - \frac{0.035}{1+\beta^3} \tag{3}$$

The coefficients $c_6 - c_1$ are: $c_6 = 0.0068$, $c_5 = 21$, $c_4 = 5$, $c_3 = 0.4$, $c_2 = 116$, and $c_1 = 0.5176$ and the tip-speed ratio (λ) can be defined as:

$$\lambda = \frac{\text{tip speed of the blade}}{\text{wind speed}} = \frac{\omega_r R}{V_w} \tag{4}$$

where R is the radius of turbine rotor (m) and ω_r is rotor speed (rad/s).

According to equations (1)–(4), the power coefficient versus tip-speed ratio ($C_p - \lambda$) curve for different values of the pitch-angle beta (β) for the employed wind turbine is obtained as shown in Figure 2.

Employed induction generator modeling

For the modeling of IG, the a-b-c reference frame is transformed into the *d-q* axis reference frame and the equivalent model is as shown in Figure 3 (Ackerman, 2015). All electrical variables and parameters are referred to the stator, where φ_{ds}, φ_{qs}, φ_{dr}, φ_{qr}, V_{ds}, V_{qs}, V_{dr}, V_{qr}, and i_{ds}, i_{qs}, i_{dr}, i_{qr} are the flux linkages, voltages, and currents of the stator and rotor in d-q reference frame, respectively.

L_{1s} and L_{1r} are the stator and rotor leakage inductances, ω_b is the base speed of the reference and ω_r is the generator rotor speed, L_s, L_r, and L_m, respectively stator, rotor, and mutual inductances. Moreover, R_s and R_r are stator and rotor resistances.

The per-unit equation of the electromagnetic torque is expressed as:

$$T_e = \varphi_{ds} i_{qs} - \varphi_{qs} i_{ds} \tag{5}$$

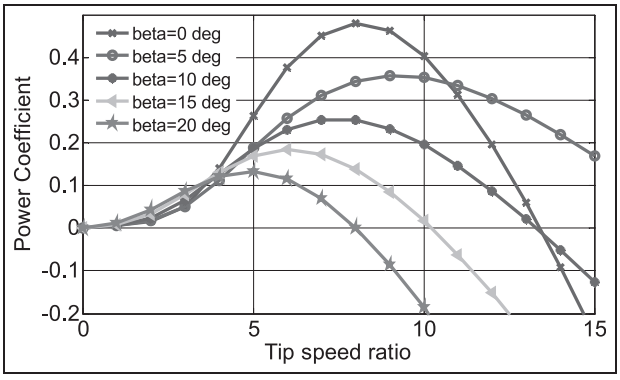

Figure 2. Wind turbine $C_p - \lambda$ curve.

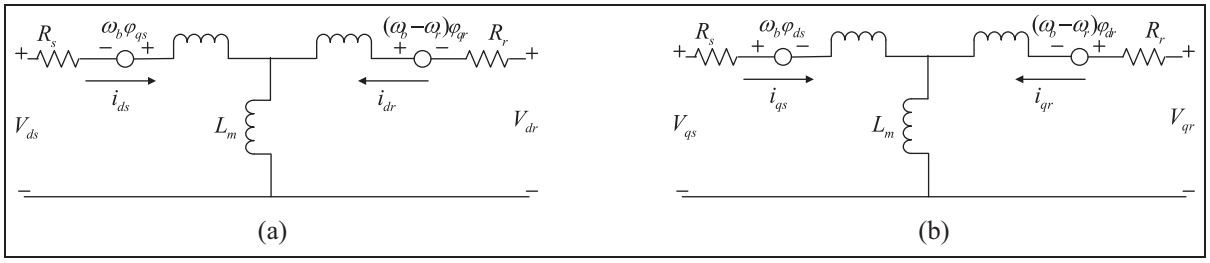

Figure 3. *d-q* reference frame of the IG: (a) *d*-axis and (b) *q*-axis.

Since generator rotor and wind turbine can be represented as an equivalent mass, the dynamic equation of motion can be written as.

$$p\omega_m = \frac{\omega_b}{2H}(T_m - T_e) \tag{6}$$

Where H is the equivalent inertia constant of both induction generator rotor and wind turbine.

Employed pitch angle control system

The block diagram of implemented pitch-angle control system for the employed wind turbine of this work is shown in Figure 4. When the wind speed crosses above rated wind speed (V_{wR}), the pitch angle controller limit the aerodynamic toque to maintain the generator output power at its rated value. The difference between the measured power (P_g) and reference power (P_g^{REF}) goes through the controller $C(s)$, which regulates the output power in accordance with error (ε), by generating suitable pitch angle.

The pitch-angle control strategy mathematically can be expressed as follows

$$\beta_c = \frac{\Delta\beta}{\Delta P}\left(P_g - P_g^{REF}\right) + \beta_i \tag{7}$$

where ΔP and $\Delta\beta$ are small-signal state variables of mechanical power and pitch angle, respectively, and β_i is initial pitch-angle.

The pitch angle (β) follows the reference pitch or optimum pitch (β_c) by a first order lag with time constant T_β, which is depends on the pitch actuator. In order to get the realistic response from the pitch control system, the pitch rate and the regulations range of pitch angle are set to $\pm 2^\circ/\text{sec}$ and $0^\circ - 45^\circ$, respectively.

Implemented PI controller design

In this work, a PI controller has designed using the linearized model of the WES where Ziegler-Nichols method (Ziegler and Nichols, 1942) is employed to determine the controller gains in an appropriate way. During the above

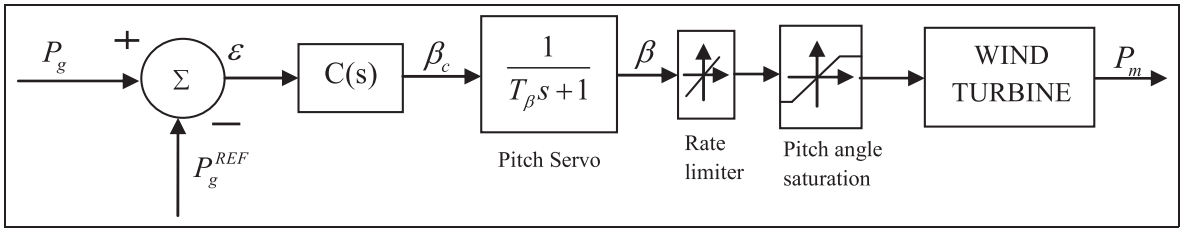

Figure 4. Implemented pitch-angle control system.

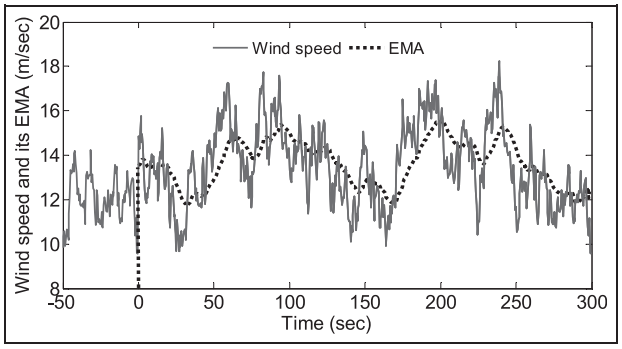

Figure 5. Comparison of wind speed and EMA.

rated wind speed, the PI controller is used to regulate the output power at its rated value by generating suitable pitch angle. But in partial load region where the wind speed is below rated, there is no pitch angle generation and PI controller extract maximum output power accordingly. But any variation in the wind speed causes high fluctuations in output power. If a large amount of wind farms are realized and hence these output power fluctuations lead to grid frequency disturbances. Therefore, the approach for smoothing the output power fluctuations is essential, as the wind farms have the capacity to minimize the output power fluctuations in partial load region.

One major challenge in wind power smoothing is setting of reference output power. Constant reference output power is not always a good choice as there may be some cases where the wind speed is below the rated wind speed and appropriate output power cannot be obtained. As a result, exponential moving average (EMA) is the best suited method to generate a reference power. Thus, in this paper EMA concept has been implemented and incorporated to the employed pitch angle controller to generate reference power.

Calculating controller reference power (P_g^{REF})

In order to obtain the output power smoothing in partial load region, an essential task is to calculate the reference power command (P_g^{REF}) of the pitch angle controller. Different approaches have been presented for determining the reference power command. However, exponential moving average (EMA) method offers better performance. The superiority of the EMA method over other approaches is that it follows wind speed quickly (Muyeen et al., 2009).

The numerical expression for EMA is given as

$$\mathrm{EMA} = [(\mathrm{C} - \mathrm{P}) \times \mathrm{K}] + \mathrm{P} \tag{8}$$

Where C is the current value, the previous period's of EMA is P, and K is weighting factor. For period based EMA, the weighting factor (K) is equal to $2/(1 + N)$, where N is the number of periods. A detailed explanation has presented in Muyeen et al. (2009). Figure 5 demonstrates the obtained average values of EMA. The EMA starts from 50 seconds (each of 1 period) when the 50 periods of data is available. However, in this paper, the average EMA values are calculated for generated wind power (not for wind speed).

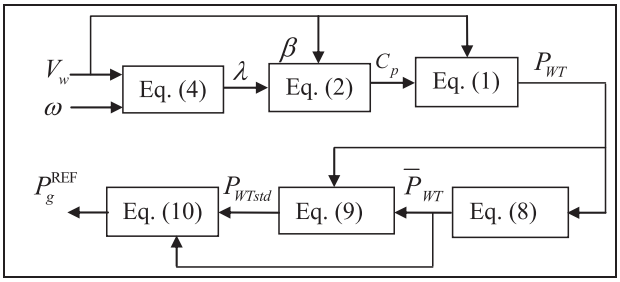

Figure 6. Computation of controller reference power command.

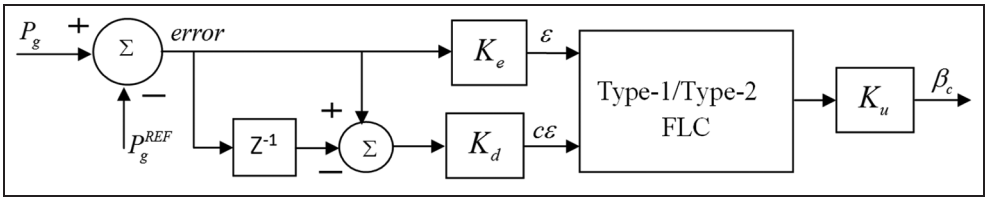

Figure 7. Proposed FLC based pitch angle controller.

The reference power command P_g^{REF} for the pitch angle controller is calculated as follows:

Step 1: The capture wind power (P_{WT}) can be obtained from equation (1).
Step 2: The average EMA value of captured wind turbine power ($\overline{P}_{WT}$) is calculated from equation (8).
Step 3: The standard deviation can be calculated as:

$$P_{WTstd} = \sqrt{\frac{\int_0^t \left(P_{WT} - \overline{P}_{WT}\right)^2 dt}{t}} \tag{9}$$

Step 4: Finally, the reference command power of controller can be obtained as

$$P_g^{REF} = \left(\overline{P}_{WT} - P_{WTstd}\right) \tag{10}$$

Figure 6 explains the whole process of reference power command calculation.

Fuzzy logic (Type-1 and Type-2) pitch angle controller design

In general pitch angle controller generate pitch angle in above rated wind speed in order to limit the output power at its rated value. In this section, a typical pitch angle controller is presented in which the wind turbine output power can be controller with pitch angle generation even when the wind speed is below rated. The employed pitch angle controller for both Type-1 and Type-2 FLC is as shown in Figure 7.

At first generator reference power command (P_g^{REF}) has obtained as explained before. The difference between P_g and P_g^{REF} is processed through the fuzzy logic controllers to generate command signal β_c. For convenience, suitable values of the scaling gains (K_e, K_d, and K_u) of the controller input and output are chosen.

Design of fuzzy logic controller (Type-1 FLC)

In 1965, Professor Lofti Zadeh has proposed the concept of fuzzy logic (FL) (Zadeh, 1965). The aim of the FL is to develop the output by allowing a set of membership rather than crisp value. It has been found to be an excellent choice for many control applications, as it mimics the human control logic. The fuzzy rules are framed on the basis

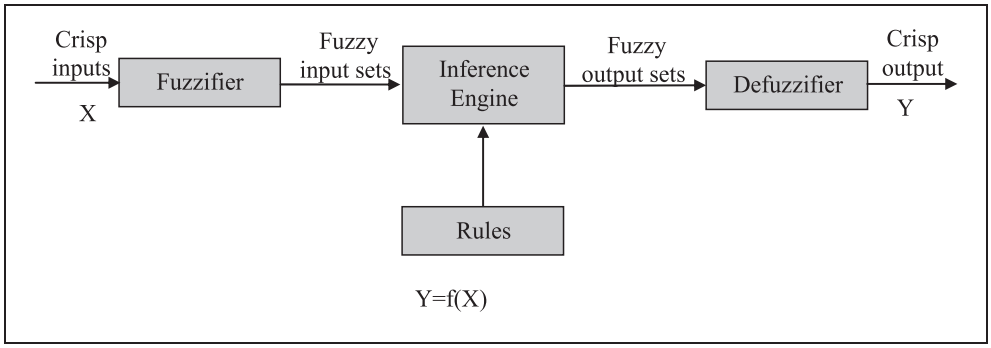

Figure 8. Schematic diagram of classical (Type-1) fuzzy logic controller.

of the expert knowledge gained upon the performance of the system over a time. The expert knowledge so gained about system output behavior is expressed in terms of membership functions of various control parameters. The block diagram of a conventional FLC (named as Type-1 FLC) is as shown in Figure 8. It consists of fuzzifier, inference engine, and defuzzifier. Here, the fuzzifier converts the crisp value of the input parameter into the fuzzy set and depending upon the fuzzy rules framed based on the membership functions for a given parameter of the system and then, fuzzy outputs are obtained with the help of the Inference Engine. In the end, defuzzifier converts these fuzzy inputs to a crisp output of the FLC to be used for the control purpose.

Proposed interval Type-2 FLC design

Quite often, the expert knowledge that is used to construct the rules in a Type-1 FLC is uncertain as the knowledge gained by different experts may or may not be the same. There are three ways in which uncertainty involved with the fuzzy rules can occur are—(1) the rules utilize the words in antecedent and consequent which can mean different things to different people (Mendel, 1999), (2) the consequents obtained from the group of experts can be different for the same rule, and (3) due to noisy training data, uncertainty in antecedent, and consequent can transfer into MFs. Therefore, Type-1 FLC, whose membership functions are Type-1 fuzzy sets are unable to handle the uncertainties in the rules. As a result, it may degrade the performance of the Type-1 FLC, especially, when the plant is subjected to the disturbances.

So as to accommodate the uncertainty involved in the expert knowledge, Type-2 FLC is a new technique which offers special features and conquers the limitations of Type-1 fuzzy sets while handling the uncertainties. The primary membership grade of a Type-2 FLC is a Type-1 fuzzy set in [0, 1] and the secondary membership is a crisp number in [0, 1] (Mizumoto and Tanaka, 1976). The secondary membership function and the range of uncertainty are decided by the third dimension of Type-2 fuzzy sets and footprint-of-uncertainty (FOU), respectively. Thus in the design of Type-2 FLC, these features can offer additional degree-of-freedom to handle various uncertainties. Hence, wind energy systems, being highly uncertain, can utilize the special features of Type-2 FLCs to improve its operational efficiency.

Elementary concept of Type-2 fuzzy sets. A Type-2 fuzzy set (denoted $\tilde{\mathrm{A}}$) with a Type-2 MF $\mu_{\tilde{\mathrm{A}}}(x,u)$ can be described as

$$\tilde{\mathrm{A}} = \left\{ \left((x,u), \mu_{\tilde{\mathrm{A}}}(x,u)\right) \;\; \forall x \in X, \forall u \in J_x \subseteq [0,1] \right\} \tag{11}$$

Where $x \in X$, $u \in J_x \subseteq [0,1]$ and $0 \leqslant \mu_{\tilde{\mathrm{A}}}(x,u) \leqslant 1$. $\tilde{\mathrm{A}}$ can also be characterized as

$$\tilde{A} = \int_{x \in X} \int_{u \in J_x \subseteq [0,1]} \frac{\mu_{\tilde{\mathrm{A}}}(x,u)}{(x,\ u)} \tag{12}$$

Where $x \in X$ and $u \in U$ are the primary and secondary variables, respectively. The secondary variable has domain J_x at each $x \in X$; J_x is called the primary membership.

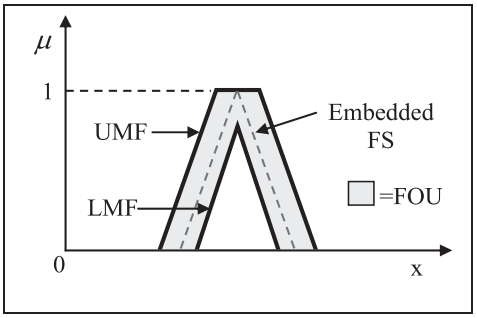

Figure 9. Type-2 fuzzy sets with FOU and embedded fuzzy set (FS).

The equation (12) means $\tilde{A} : X \rightarrow \{[a, b] : 0 \leqslant a \leqslant b \leqslant 1\}$. The union of all the primary memberships is called the footprint-of-uncertainty (FOU) of $\tilde{A}$ and is shown as the shaded region of Figure 9.

$$FOU\left(\tilde{A}\right) = \cup_{\forall x \in X} J_x = \{(x, u) : u \in J_x \subseteq [0, 1]\} \tag{13}$$

The FOU of Type-2 fuzzy set (Ã) has bounded by two Type-1MFs called as lower membership function (LMF) and the upper membership function (UMF). The UMF and LMF are denoted as $\bar{\mu}_{\tilde{A}}(x)$ and $\underline{\mu}_{\tilde{A}}(x)$, respectively, and are defined as follow:

$$\bar{\mu}_{\tilde{A}}(x) = \overline{FOU(\tilde{A})} \qquad \forall_{x \in X} \tag{14}$$

$$\underline{\mu}_{\tilde{A}}(x) = \underline{FOU(\tilde{A})} \qquad \forall_{x \in X} \tag{15}$$

Note that J_x is an interval set; that is,

$$J_x = \{(x, u) : u \in \left[\underline{\mu}_{\tilde{A}}(x), \overline{\mu}_{\tilde{A}}(x)\right]\}, \tag{16}$$

An embedded fuzzy set (FS) $\tilde{A}_e$ for a continuous universe of discourse X and u is expressed as

$$\tilde{A}_e = \int_{x \in X} [1/u]/x, \qquad u \in J_x \tag{17}$$

The set $\tilde{A}_e$ is embedded in $\tilde{A}$ in such a way that the secondary MF is always one at each value of x. A large number of such embedded Type-1 fuzzy set (FS) are combined to form the Type-2 FS. According to Qilian and Mendel (2000) the Type-2 FS can be considered as a combination of many different Type-1 FSs where each Type-1 FS is embedded to form the FOU.

Designing algorithm of Type-2 FLC for the studied WES. The Figure 10 shows the steps involved in the Type-2 FLC design algorithm.

At first, with help of various membership functions the crisp input is converted to fuzzy inputs using Type-2 membership functions of various system parameters so as to account for the uncertainty involved in the expert knowledge. Then using logical operators, a set of fuzzy rules have been framed to combine the fuzzy output sets into a single set under the inference mechanism. The output of inference engine is converted to Type-1 under Type reduction operation and then, the Type reduced sets are converted back to crisp value using various defuzzification techniques as done in the Type-1 FLC. The detailed procedure of designing the Type-2 FLC of the given wind energy systems is as follows:

The MFs and rules are framed for the Type-1 and Type-2 FLCs as given in Figure 11 and Table 1, respectively. The triangular MFs with overlap used for the input and output fuzzy sets. For all the inputs and outputs the universe of discourse is chosen as $[-1, +1]$.

Fuzzification. As shown in the schematic diagram of the controller configuration (Figure 7), the input and output variables used for the controller design are expressed with the help of fuzzy sets using seven triangular linguistic

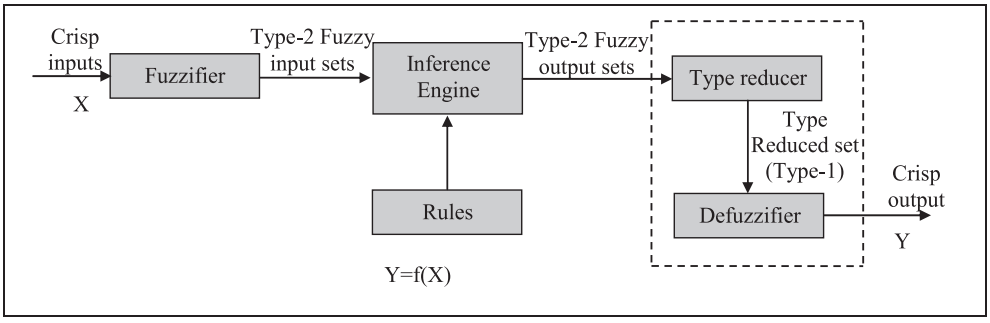

Figure 10. Schematic diagram of Type-2 FLC.

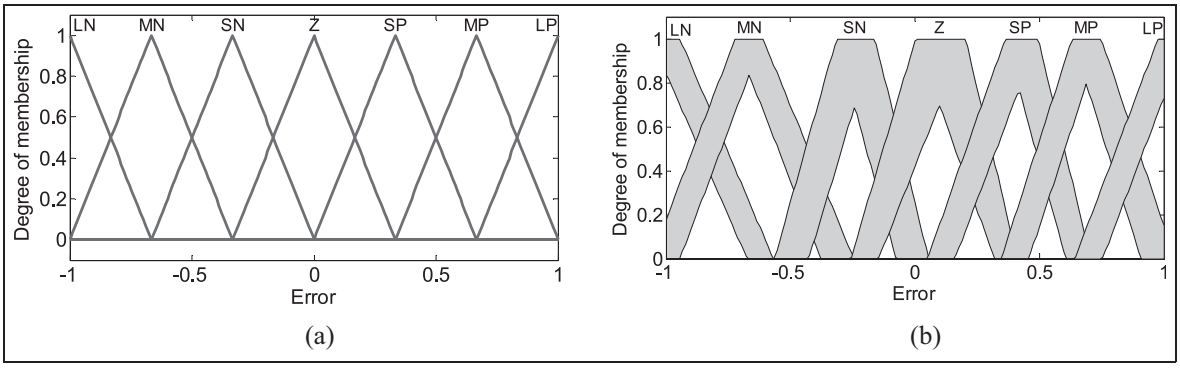

Figure 11. Designed MFs of inputs and output: (a) Type-1 FLC–inputs (ε and $c\varepsilon$) and output (β_c) and (b) Type-2 FLC–inputs (ε and $c\varepsilon$) and output (β_c).

variables MFs. Notation for the fuzzy sets as: LP (Large Positive), MP (Medium Positive), SP (Small Positive), Z (Zero), SN (Small Negative), MN (Medium Negative), LN (Large Negative). The MFs are selected based on prior knowledge and observations from the various simulation results. The width of the FOU is decided by observing its effect on the WES output power oscillations. The similar MFs and rules have been designed for Type-1 and Type-2 FLCs to distinguish their performance subjected to below rated wind speed disturbances.

Fuzzy logic rules/inference engine. The major function in the inference engine is the rules' implementation, aggregation, and Type reduction. With help of the experts' knowledge on the pitch-angle control of the wind energy system, a control strategy is framed as a set of IF-THEN rules and are as:

If (ε is x_1) and ($c\varepsilon$ is y_1) then (β_c is w_1)

Similarly, 49 rules have been defined for all input-output MFs as shown in Table 1. In the Type-2 FLCs, the union and intersection functions are defined by join and meet operations to map the input and output sets with fired rules. Therefore, the inference engine utilizes respectively, min-method and max-method for meet and join operations, respectively. Using the extension principle, a detailed mathematical relation between the meet and join operations has presented in Mizumoto and Tanaka (1976). During the aggregation operation, all the fired rules are converted to become a single output fuzzy set. However, the output of inference engine cannot be converted directly to crisp value due to computational limitations. As a result, Type reduction (TR) method has been suggested in the Type-2 FLC system to convert from Type-2 output fuzzy sets to Type-1 fuzzy sets first, and thereafter the normal defuzzification techniques can be applied. Height, center-of-sets, center-of-sums, and modified-height are the most accepted TR methods (Karnik and Mendel, 1999), in which centroids of the embedded Type-2 sets are calculated. If larger the FOU width, the number of embedded fuzzy sets increases and this leads to increase in the computational time of TR method. In the present work "height" TR method has been used for the calculation of the centroid of Type-2 FLCs as it involves much lesser computations as compared to other methods (Karnik and Mendel, 1999).

Table 1. Fuzzy rules table for (β_c).

Change in error ($c\varepsilon$)	Error (ε)						
	LN	MN	SN	Z	SP	MP	LP
LN	LN	LN	LN	LN	MN	SN	Z
MN	LN	LN	LN	LN	SN	Z	SP
SN	LN	LN	MN	MN	Z	SP	MP
Z	LN	MN	SN	Z	SP	MP	LP
SP	MN	SN	Z	MP	MP	LP	LP
MP	SN	Z	SP	MP	LP	LP	LP
LP	Z	SP	MP	LP	LP	LP	LP

Defuzzification. The common defuzzification methods used for the Type-2 FLC are the first (or last) of maxima, centroid-of-area, and mean-of-max methods. In this study, centroid-of-area method has been utilized which is the most reasonable and popular method among the others. The centroid of the Type-2 fuzzy set is the collection of centroids of all of its embedded sets. The defuzzification method converts the output fuzzy to crisp value. The final output of the controller is defined as

$$\beta^* = \frac{1}{T_\beta s + 1}\beta_c^{'} \tag{18}$$

$$\text{Where } \beta_c^{'} = \frac{\Delta\beta}{\Delta P}\left(P_{elec} - P_{ref}\right) + \beta_i$$

The starred value is the final output of the pitch controller, whereas the prime term is the outputs of the Type-2 fuzzy controller.

Real time simulation

The real time simulation of the studied system is carried-out on OPAL-RT digital simulator. The RT-lab, which is fully integrated with MATLAB/Simulink®, provides the flexibility and scalability to achieve the most complex real-time simulation applications in the power systems, power electronics, automotive, aerospace, and industries (Mikkili and Panda, 2013; RT-LAB, 2019; Venne et al., 2010). The simulator uses advanced fixed-time step solvers (ARTEMIS) for strict constraints of real-time simulation of stiff systems. The sampling time used to realize the system is $50\mu s$. To run the models in real-time simulation, the RT-lab allows user to readily converted Simulink models through real-time workshop (RTW). The steps involved in implementation of MATLAB/Simulink model to real-time have been provided in detail in Mikkili et al., (2015). The RT-lab can separate a complex system into simple sub-systems and performs parallel operation in multiple cores. Hence, one needs to separate the model into suitable sub-systems for real time simulation Zhao et al. (2012). The studied WES as shown in Figure 1 can be divided into two sub-systems as shown in Figure 12. The console subsystem denoted as SC_Console which contains parameters accessing and displaying blocks. This sub-system runs on the host PC, which can receive simulation results and display through the scope. Another sub-system is a computing sub-system named as SM_Master which contains all the calculation blocks (of studied WES). This sub-system runs on the target machine with real-time condition.

The real-time digital simulation laboratory setup is as shown in Figure 13; it consists of host personal computer (Host-PC), target (real-time digital simulator), and oscilloscope. The simulator employed here is OP5600 with one processor and four 3.33-GHz dedicated cores to perform parallel computations. The work station computer (Host-PC) executes the WES model and interacts with the real-time digital simulator (RTDS) to produce the results of real-time simulation. The digital oscilloscope is also employed to observe the real-time results of pitch angle generation.

The results of Type-2 FLC are compared with Type-1 FLC and PI controller used, one at a time, for pitch controller. The performance of the proposed controller is tested for below rated wind speed disturbances since the power smoothing can be done in this region.

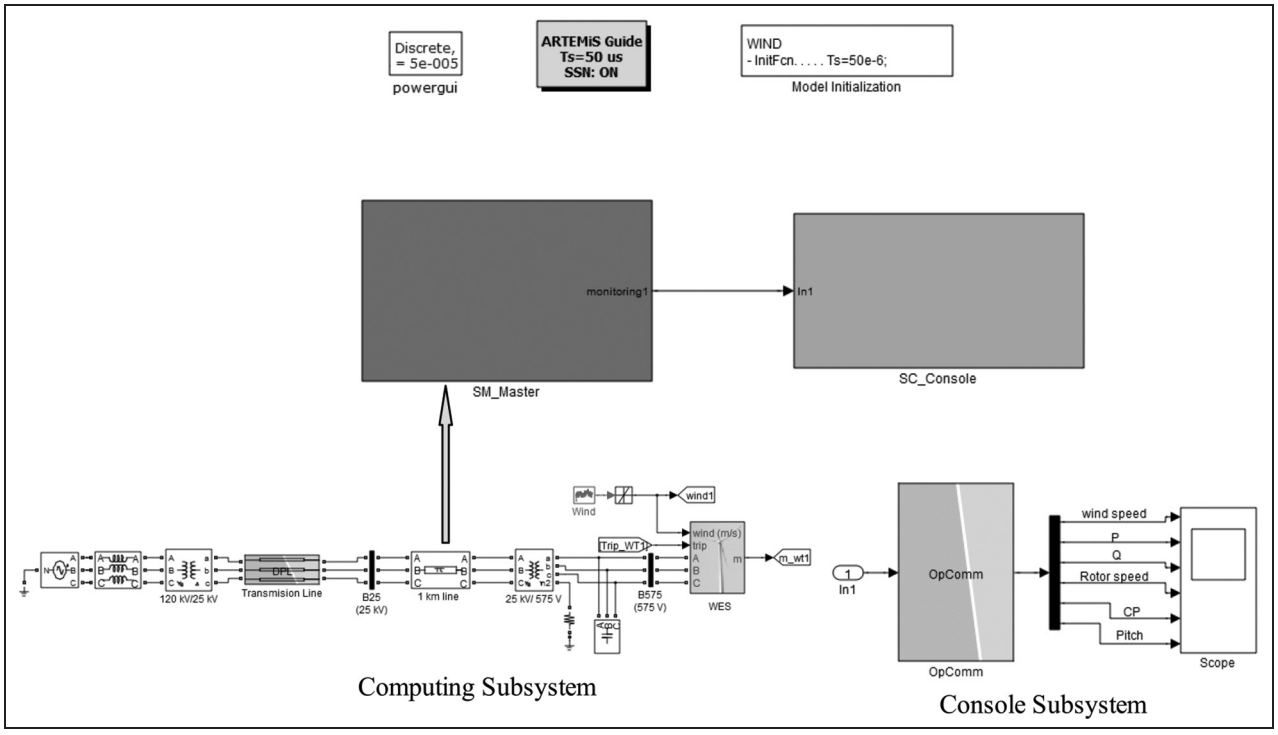

Figure 12. Distributed model of the WES for real time simulation.

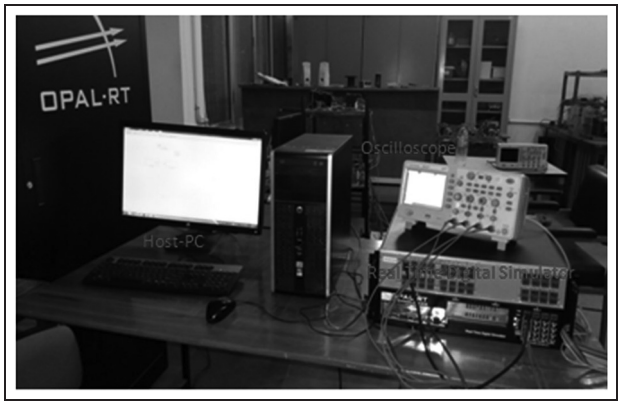

Figure 13. Hardware implementation of studied system.

The wind speed pattern considered for partial load region (below rated wind speed) is as shown in Figure 14. Under this wind speed characteristics, the performance of the PI, Type-1 FLC, and the proposed Type-2 FLC was investigated and the real-time simulation results were obtained through opcomm block for generator active power, generator rotor speed, power coefficient, and pitch angle are as shown in Figures 15 to 18, respectively. When the wind speed is below rated value, there is no pitch angle generated with PI controller which ensures no point of limiting the rotor speed and the wind turbine operates with its maximum possible power extraction. As a result, the generator active and rotor speed followed the wind speed disturbances and exhibits huge fluctuations (see Figures 15 and 16). If these fluctuating power exported to grid causes grid frequency to fluctuate.

Thus, it is needed to smoothen out these power fluctuations. For smoothing the output power fluctuations, at first it is required to determine the reference power command (P_g^{REF}) as discussed in the previous sub-section 3.2 and thereafter, fuzzy logic approaches (Type-1 and Type-2 FLC) are implemented. These FLCs are good at tracking reference power (command power) irrespective of system operating conditions by generating a suitable pitch-angle. On comparing, it is observed from Figure 15 that the active power output of the wind energy system follows

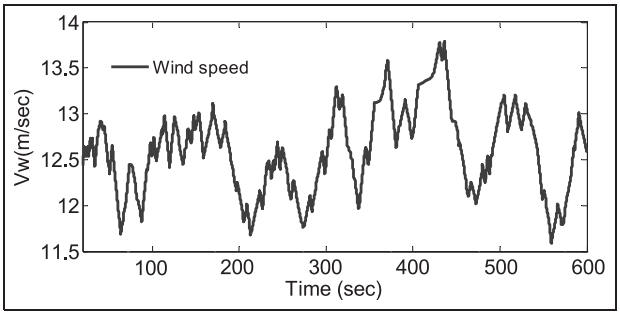

Figure 14. Below rated wind speed profile.

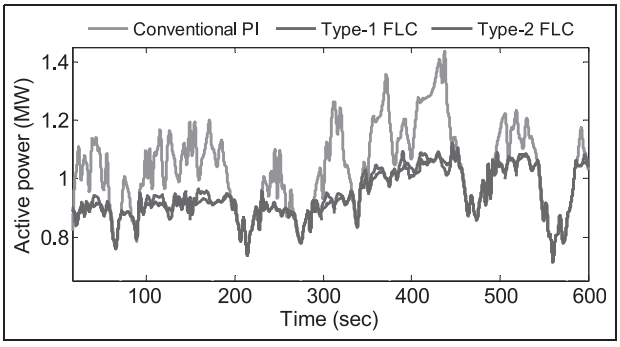

Figure 15. Generator active power.

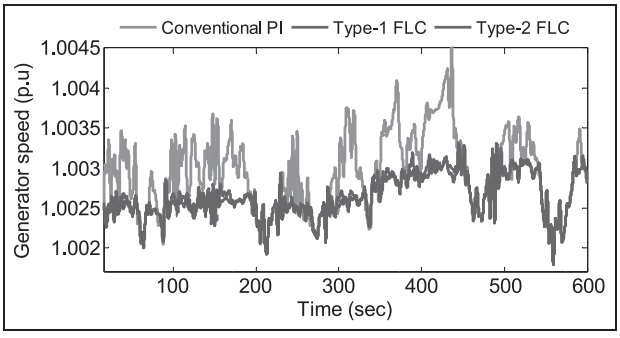

Figure 16. Generator rotor speed.

the command output power with small variations with Type-1 and Type-2 controllers but real power fluctuations are being smoothened more effectively by the Type-2 FLC pitch-angle controller. The similar results are also seen with generator rotor speed too, it has been more efficiently smoothen out by the proposed controller as shown in Figure 16. The power-coefficient of wind turbine with conventional PI, Type-1, and Type-2 FLCs controllers are as shown in Figure 17. The power-coefficient with PI controller is always maintained at its maximum value of 0.48, since there is no pitch angle generation. However, with Type-1 and Type-2 FLCs, the power-coefficient varies according to the pitch-angle variations in order to smoothing the output power. The pitch-angle profiles of the WES with all employed controllers are as shown in Figure 18. The pitch controller action with conventional PI, Type-1, and Type-2 FLCs are also observed in the digital oscilloscope and depicted in Figure 19(a) to (c). As there is no pitch angle generation with PI controller thus straight line (zero) has been observed in oscilloscope (see Figure 19(a)). But with Type-1 and Type-2 FLCs pitch-angle activity has been achieved and recorded in the digital oscilloscope as shown in Figure 19(b) and (c), respectively.

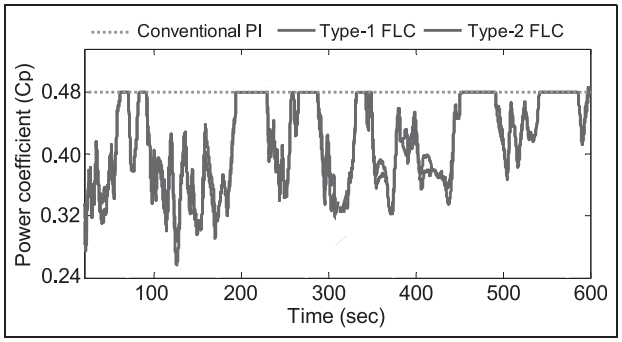

Figure 17. Power coefficient.

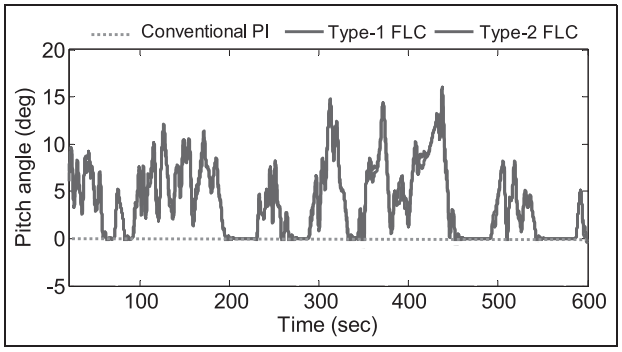

Figure 18. Pitch angle generation by different controllers.

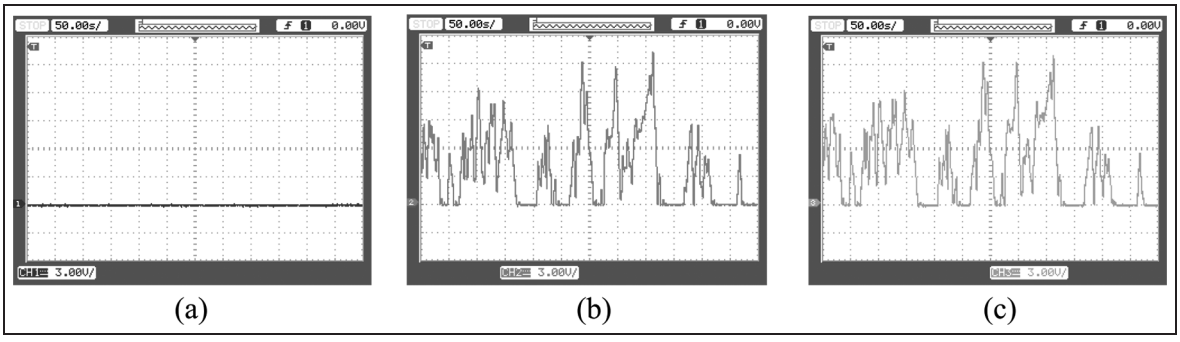

Figure 19. Pitch angle profile obtained in oscilloscope: (a) PI controller, (b) Type-1 FLC, and (c) Type-2 FLC.

To estimate the performance of the proposed technique (Type-2 FLC) with PI and Type-1 FLC, the output power smoothing P_{smooth} and maximum energy ($W_{\max}$) functions are calculated as Senjyu et al. (2006):

$$P_{smooth} = \int_0^T \left| \frac{dP_g(t)}{dt} \right| dt \tag{19}$$

$$W_{\max} = \int_0^T P_g(t) dt \tag{20}$$

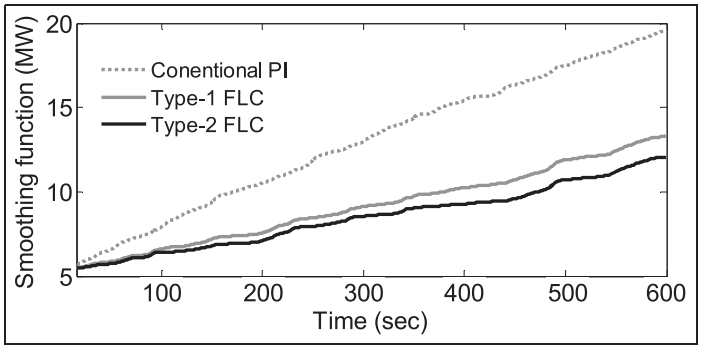

Figure 20. Output power smoothing function.

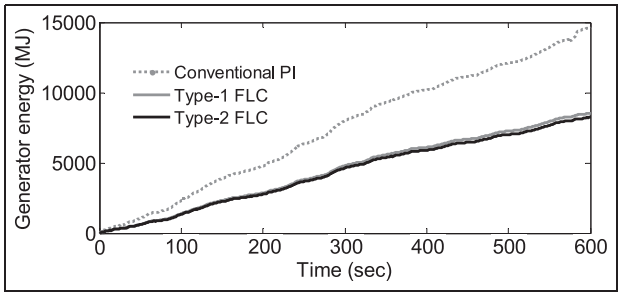

Figure 21. Maximum energy function.

Where P_g is the generated output power and T is the total simulation time. In equation (19)P_{smooth} is the integral of the absolute value for the differentiation of the generated output power P_g. Thus if P_{smooth} is small, the generated power fluctuation of the wind energy system is small, as a result, the studied system exhibiting good performance.

Figure 20 shows that the power smoothing function with Type-2 FLC method has smaller magnitude compared to PI and Type-1 FLC throughout the simulation time. Since the slope of the Type-2 FLC is small compared to other methods, therefore, if the studied wind energy system is integrated into a small-island (such as a small capacity-power system), the proposed method can also be validated for frequency fluctuations.

Figure 21 shows the energy function obtained with all the controllers. The maximum energy has been obtained with a conventional PI controller as there is no pitch angle generation it remains fixed at 0°. But with Type-1 and Type-2 FLCs there is a drop in the output power due to pitch angle generation. The purpose of this work is to smooth the output power and thus drop cannot be avoided. From the Figure 21, the percentage of drop during the 600 seconds for Type-1 and Type-2 FLCs are calculated with respect to PI controller. The energy loss of Type-1 and Type-2 FLC with respect to a conventional PI controller is respectively, 30.02% and 30.31% approximately.

Conclusions

Concerning the generator output power smoothing, a Type-2 FLC based pitch-angle controller is proposed for WES when it subjected to varying wind speed. At first, reference power command based on EMA concept is obtained and then, fuzzy controllers (Type-1 and Type-2) are implemented to follow the reference power command. To validate the present work, the studied system has designed in MATLAB/Simulink and then exported to RT-lab via RTW for real time simulation. The below rated wind speed pattern is employed to study the effectiveness of the proposed controller. The simulation results show the pitch-angle controller with Type-2 FLC offers better performance in smoothing the output power of WES than PI and Type-1 FLC. To estimate the smoothing level of proposed controller, power smoothing function (index) has been incorporated. Due to good output power smoothing achieved with proposed controller, the system frequency which is affected with power fluctuations can be controlled within the acceptable limit.

Declaration of conflicting interests

The author(s) declared no potential conflicts of interest with respect to the research, authorship, and/or publication of this article.

Funding

The author(s) received no financial support for the research, authorship, and/or publication of this article.

ORCID iD

Kanasottu Anil Naik https://orcid.org/0000-0002-3321-5097

References

Ackermann T (2005) *Wind Power in Power System*. Hoboken, NJ: John Wiley & Sons.

Cardenas R, Pena R, Asher G, et al. (2004) Power smoothing in wind generation systems using a sensorless vector controlled induction machine driving a flywheel. *IEEE Transactions on Energy Conversion* 19: 206–216.

Chowdhury MA, Hosseinzadeh N and Shen WX (2012) Smoothing wind power fluctuations by fuzzy logic pitch angle controller. *Renewable Energy* 38: 224–233.

Duong MQ, Grimaccia F, Leva S, et al. (2014) Pitch angle control using hybrid controller for all operating regions of SCIG wind turbine system. *Renewable Energy* 70: 197–203.

Hagras H and Wagner C (2012) Towards the wide spread use of type-2 fuzzy logic systems in real world applications. In: *IEEE computational intelligence magazine*, August 2012, vol. 7, pp.14–24. New York: IEEE.

Haque MH (2014) Evaluation of power flow solutions with fixed speed wind turbine generating systems. *Energy Conversion and Management* 79: 511–518.

Kamel RA, Chaouachi A and Nagasaka K (2010) Wind power smoothing using fuzzy logic pitch controller and energy capacitor system for improvement Micro-Grid performance in islanding mode. *Energy* 35: 2119–2129.

Karnik NN and Mendel JM (1999) Type-2 fuzzy logic systems. *IEEE Transactions on Fuzzy* 7: 643–658.

Kinjo T, Senjyu T, Uezato K, et al. (2006) Output leveling of wind power generation system by EDLC Energy storage system. *Electrical Engineering in Japan* 154: 34–41.

Mendel JM (1999) Computing with words when words can mean different things to different people. In: *Proceedings of third international ICSC symposium on fuzzy logic and applications*, pp.1–7. Rochester, NY: Rochester Institute of Technology.

Mendel JM, John RI and Liu F (2006) Interval type-2 fuzzy logic systems made simple. *IEEE Transactions on Fuzzy Systems* 14: 808–821.

Mikkili S and Panda AK (2013) Types-1 and -2 fuzzy logic controllers-based shunt active filter Id–Iq control strategy with different fuzzy membership functions for power quality improvement using RTDS hardware. *IET Power Electronics* 6(4): 818–833.

Mikkili S, Panda AK and Prattipati J (2015) Review of real-time simulator and the steps involved for implementation of a model from MATLAB/SIMULINK to real-time. *Journal of the Institution of Engineers (India): Series B* 96(2): 176–196.

Mizumoto M and Tanaka K (1976) Some properties of fuzzy sets of type 2. In: *2008 international conference on machine learning and cybernetics*, Kunming, China, 12–15 July 1976, vol. 31, pp.312–340. New York: IEEE.

Muyeen SM, Ali MH, Takahashi R, et al. (2007) Wind generator output power smoothing and terminal voltage regulation by using STATCOM/ESS. In: *IEEE Power Tech*, Lausanne, Switzerland, 1–5 July 2007, pp.1232–1237. New York: IEEE.

Muyeen SM, Shishido S, Ali MH, et al. (2008) Application of energy capacitor system to wind power generation. *Wind Energy* 2008: 11: 335–350.

Muyeen SM, Tamura J and Murata T (2009) *Stability Augmentation of a Grid Connected Wind Farm*. London: Springer-Verlag London Ltd.

Qilian L and Mendel JM (2000) Interval type-2 fuzzy logic systems: Theory design. *IEEE Transactions on Fuzzy Systems* 8: 535–550.

RT-LAB (2019) *RT-LAB Version 10.7.0.361 User Guide, Opal-RT*. Uttarakhand, India: IIT Roorkee.

Sakamoto R, Senjyo T, Kaneko T, et al. (2006) Output power leveling of wind turbine generator by pitch angle control using H-∞ control. In: *2006 IEEE PES power systems conference and exposition*, Atlanta, GA, 29 October–1 November 2006, pp.1–6. New York: IEEE.

Sakamoto R, Senjyu T, Kinjo T, et al. (2004) Output power leveling of wind turbine generator by pitch angle control using adaptive control method. In: *2004 international conference on power system technology*, 2004. PowerCon, 21–24 November 2004, 834–839. New York: IEEE.

Senjyu T, Sakamoto R, Kaneko T, et al. (2008) Output power leveling of wind farm using pitch angle controller with fuzzy neural networks. In: *2006 IEEE power engineering society general meeting*, Montreal, QC, 2008, vol. 36, pp.1048–1066. New York: IEEE.

Senjyu T, Sakamoto R, Urasaki N, et al. (2006) Output power leveling of wind turbine generator for all operating regions by pitch angle control. In: *IEEE transactions on energy conversion*, June 2006, vol. 21, no. 2, pp.467–475. New York: IEEE.
Sheikh MRI, Muyeen SM, Takahashi R, et al. (2011) Smoothing control of wind generator output fluctuations by PWM voltage source converter and chopper controlled SMES. *European Transactions on Electrical Power* 21: 680–697.
The Global Wind Energy Council Belgium (2016) http://www.gwec.net/global-Fig.s/wind-in-numbers/ (accessed 5 August 2017).
Venne P, Paquin JN and Belanger J (2010) The what, where and why of real-time simulation. In: *Proceedings of the power and energy society general meeting*, Minneapolis, Minnesota, 1–4th October, 2010, pp. 37–49. USA: PES.
Yin X (2018) An up to date review of continuously variable speed wind turbines with mechatronic variable transmissions. *International Journal of Energy Research* 42(4): 1442–1454.
Yin X, Lin YG and Li W (2016) Predictive pitch control of an electro-hydraulic digital pitch system for wind turbines based on the extreme learning machine. *Transactions of the Institute of Measurement and Control* 38(11): 1392–1400.
Yin X, Lin YG and Li W (2017) Modeling and loading compensation of a rotary valve-controlled pitch system for wind turbines. *Journal of Zhejiang University-SCIENCE A* 18(9): 718–727.
Yin X, Lin YG, Li W, et al. (2014a) Output power control for hydro-viscous transmission based continuously variable speed wind turbine. *Renewable Energy* 72: 395–405.
Yin X, Lin YG, Li W, et al. (2014b) Integrated pitch control for wind turbine based on a novel pitch control system. *Journal of Renewable and Sustainable Energy* 6(4): 1–20.
Yin X, Lin YG and Li W (2015a) Operating modes and control strategy for megawatt-scale hydro-viscous transmission-based continuously variable speed wind turbines. *IEEE Transactions on Sustainable Energy* 6(4): 1553–1564.
Yin X, Lin YG, Li W, et al. (2015b) A novel fuzzy integral sliding mode current control strategy for maximizing wind power extraction and eliminating voltage harmonics. *Energy* 85: 677–686.
Yin X, Lin YG, Li W, et al. (2015c) Sliding mode voltage control strategy for capturing maximum wind energy based on fuzzy logic control. *International Journal of Electrical Power & Energy Systems* 70: 45–51.
Yin X, Lin YG, Li W, et al. (2015d) Fuzzy-logic sliding-mode control strategy for extracting maximum wind power. *IEEE Transactions on Energy Conversion* 30(4): 1267–1278.
Yin X, Lin YG, Li W, et al. (2015e) Design, modeling and implementation of a novel pitch angle control system for wind turbine. *Renewable Energy* 81: 599–608.
Yin X, Lin YG, Li W, et al. (2015f) Adaptive back-stepping pitch angle control for wind turbine based on a new electro-hydraulic pitch system. *International Journal of Control* 88(11): 2316–2326.
Yin X, Lin YG, Li W, et al. (2015g) Adaptive sliding mode back-stepping pitch angle control of a variable-displacement pump controlled pitch system for wind turbines. *ISA Transactions* 58: 629–634.
Yin X, Lin YG, Li W, et al. (2016) Hydro-viscous transmission based maximum power extraction control for continuously variable speed wind turbine with enhanced efficiency. *Renewable Energy* 87: 646–655.
Yin X, Lin YG, Li W, et al. (2017) Loading system and control strategy for simulating wind turbine loads. *Journal of Vibration and Control* 23(11): 1739–1752.
Zadeh LA (1965) Fuzzy sets. *Information and Control* 8: 338–353.
Zhang L, Shen C, Crow ML, et al. (2005) Performance indices for the dynamic performance of FACTS and FACTS with energy storage. *Electric Power Components and Systems* 33: 299–314.
Zhao Y, Shi L, Ni Y, et al. (2012) Modeling and real-time simulation of wind farm. In: *2012 Asia-Pacific power and energy engineering conference*, Shanghai, China, 27–29 March 2012; pp.1–4. New York: IEEE.
Ziegler JG and Nichols NB (1942) Optimum settings for automatic controllers. *Transactions of the ASME* 65: 433–444.

Appendix 1

System parameters

Table A1. Wind turbine parameters.

Parameters	Values
Rated power	1.5 MW
Rotor diameter	64 m
Number of blades	3
Cut-in wind speed (V_{wCI})	4 m/s
Cut-out wind speed (V_R)	25 m/s
Rated wind speed (V_{wR})	14 m/s
Generator	SCIG

Table A2. SCIG generator parameters (Haque, 2014).

Parameters	Values
P_{rated}, V_{rated}	1.5 MW, 0.69 kV
R_s, R_r	0.004843 p.u., 0.004377 p.u.
L_s, L_r	0.1248 p.u., 0.1791 p.u.
L_m, H	6.77 p.u., 5.04
C	200 kVAR